BELLCOMM, INC.
955 L'ENFANT PLAZA NORTH, S.W., WASHINGTON, D.C. 20024

COVER SHEET FOR TECHNICAL MEMORANDUM

TITLE- Docking Dynamics Simulation for AAP

TM- 69-1022-6

FILING CASE NO(S)- 620

DATE- July 24, 1969

AUTHOR(S)- R. J. Ravera

FILING SUBJECT(S)
(ASSIGNED BY AUTHOR(S))- Spacecraft Docking Dynamics
Apollo Applications Program

ABSTRACT

An analytical simulation of docking dynamics of two rigid bodies that use the Apollo probe and drogue has been developed. The object of this simulation, called SDØCK, is to analyze a variety of docking problems and obtain accurate trends in a short time. The basic simplicity of the analysis (impulse momentum techniques) and the inherent assumptions lead to some loss of accuracy. However, agreement with more sophisticated analyses and tests is good. Moreover, SDØCK requires on the order of one hundredth of the computer time used by the more complex simulations. SDØCK is flexible enough to include various coefficients of restitution and friction between the probe and drogue, attitude control of the chase and target vehicles, and axial thrusting of the chase vehicle after initial contact.

Axial docking of the CSM to the AAP Cluster was simulated on SDØCK for a total of 540 sets of initial contact conditions. Each set of initial conditions was run with the following options: attitude control on the CSM without axial thrust; CSM attitude control and axial thrust; and CSM axial thrust without attitude control. Hence 1620 cases were run, requiring about 19.5 minutes on the UVIVAC 1108. The principal results of this study are as follows:

It appears that without axial thrust, miss distances of greater than 0.25 ft will be detrimental to capture.

The use of axial thrust on the chase vehicle offers significant improvement in capture probability, especially if the axial thrusters do not have to be shared with attitude control demands.

High probe tip velocity components normal to the drogue surface should be avoided.

BA-145A (8-68)

DISTRIBUTION

COMPLETE MEMORANDUM TO

CORRESPONDENCE FILES:

OFFICIAL FILE COPY
plus one white copy for each
additional case referenced

TECHNICAL LIBRARY (4)

NASA Headquarters

H. Cohen/MLR
P. E. Culbertson/MLA
W. B. Evans/MLO
L. K. Fero/MLV
J. P. Field, Jr./MLP
T. A. Keegan/MA-2
M. Savage/MLT
W. C. Schneider/ML

Bellcomm

F. G. Allen
A. P. Boysen
K. R. Carpenter
D. R. Hagner
W. G. Heffron
B. T. Howard
J. Z. Menard
I. M. Ross
J. W. Timko
R. L. Wagner
Departments 2031, 2034 Supervision
All Members Division 102
Center 10 File
Central File
Department 1024 File
Library

COMPLETE MEMORANDUM TO (Cont'd)

MSC

J. Barneburg/ES2
L. A. Bernardi/KS
L. T. Chauvin/ES12
H. W. Dotts/KS
W. H. Hamby/KM
B. W. Holder/ES3
J. A. Schliesing/ES3

MSFC

T. Bullock/R-P&VE-SLR
D. Germany/I-I/IB-E
G. B. Hardy/PM-AA-EA
W. Holland/R-P&VE-SLR
G. F. McDonough/R-SE-A

MDAC-ED

J. Dick
R. A. Garrett
P. Heaton

MMC

E. F. Bjoro
C. Bodley
G. Morosow
G. C. Pfaff

SUBJECT: Docking Dynamics Simulation for AAP   DATE: July 24, 1969
Case 620

FROM: R. J. Ravera

TM-69-1022-6

TECHNICAL MEMORANDUM

INTRODUCTION

This memorandum describes a two-dimensional analytical simulation of the docking dynamics of two rigid bodies that use the Apollo probe and drogue docking system. Given the spacecraft mass properties and a set of initial contact conditions, the simulation has the capability to predict whether a docking maneuver is a success (capture) or a failure (miss) and an estimate of the contact loads that occur during the attempt. If the attempt is successful, a good measure of the time from first contact to capture can be computed. If the attempt is a failure, the residual momentum of the spacecraft can be determined in order to give a quantitative measure of attitude control system requirements necessary for restabilization. The simulation has been used to obtain such results for docking maneuvers of Apollo Applications Program Spacecraft.

The present simulation, called SDØCK, is not nearly as elaborate as some simulations now in existence.[1,2,3] However, the more complicated simulations require from about seven seconds[1] to 24 seonds[3] of machine time for every second of real time,[1] which can mean computer runs on the order of minutes for each set of initial conditions analyzed. SDØCK can evaluate 24 cases in about 20 seconds. The trade-off between SDØCK and its more sophisticated counterparts involves low speed with more accuracy versus high speed with less accuracy. The advantages of SDØCK are that a large number of cases can be analyzed and that accurate trends can be quickly produced. Furthermore, greater selectivity of cases to be run on the more sophisticated simulations can be obtained if SDØCK is used first to identify problem cases.

DESCRIPTION OF THE SIMULATION

SDØCK, is based on impulse-momentum relationships.*[4] The analysis takes account of the effects of five initial contact conditions, friction between the probe and drogue,

---

* See the Appendix for details of the analysis.

energy loss due to permanent deformation (coefficient of restitution), attitude control of the chase vehicle, and thrusting of the chase vehicle immediately after initial contact. All motion is considered to take place in a plane; the drogue is therefore envisioned as a trough with two distinct walls rather than a conical surface. The probe tip is constrained to lie on or within these walls during a docking attempt. The following sections describe the method of treating the various components of the simulation.

A.   Initial Conditions

Due to the assumption of plane motion, only five quantities are needed to describe the initial contact conditions; these are v_A, v_L, and ω, respectively the initial axial, lateral and angular velocities of the chase vehicle with respect to the target vehicle, the offset angle, θ, and the offset distance, d (see Figure 1). The following permissible ranges of these quantities are set by Program Specification.[5]

v_A (ft/sec)	0.1 -	1.0
v_L (ft/sec)	0.0 -	$\pm$ 0.5
ω (deg/sec)	0.0 -	$\pm$ 1.0
d (ft)	0.0 -	$\pm$ 1.0
θ (deg)	0.0 -	$\pm$10.0

A given set of these quantities constitutes a case.

B.   Impact

The values of linear and angular velocities after impact are related to the initial conditions through the basic impulse-momentum relationships. The initial velocity of the probe tip relative to the drogue is computed in components normal (compression rate) and tangential (slip rate) to the drogue surface. The compression rate, slip rate and coefficients of friction and restitution* are placed into a fairly complex algorithm to determine the values of the normal and friction impulses, denoted respectively by N* and F*. In order to compute N* and F*, the algorithm must determine whether there is sufficient

---

* Evidence of permanent deformation is apparent in Reference 6.

CHASE VEHICLE

V_L

CM

ω

V_A

θ

V_A — AXIAL VELOCITY

V_L — LATERAL VELOCITY

ω — ANGULAR RATE

θ — ANGULAR OFF-SET
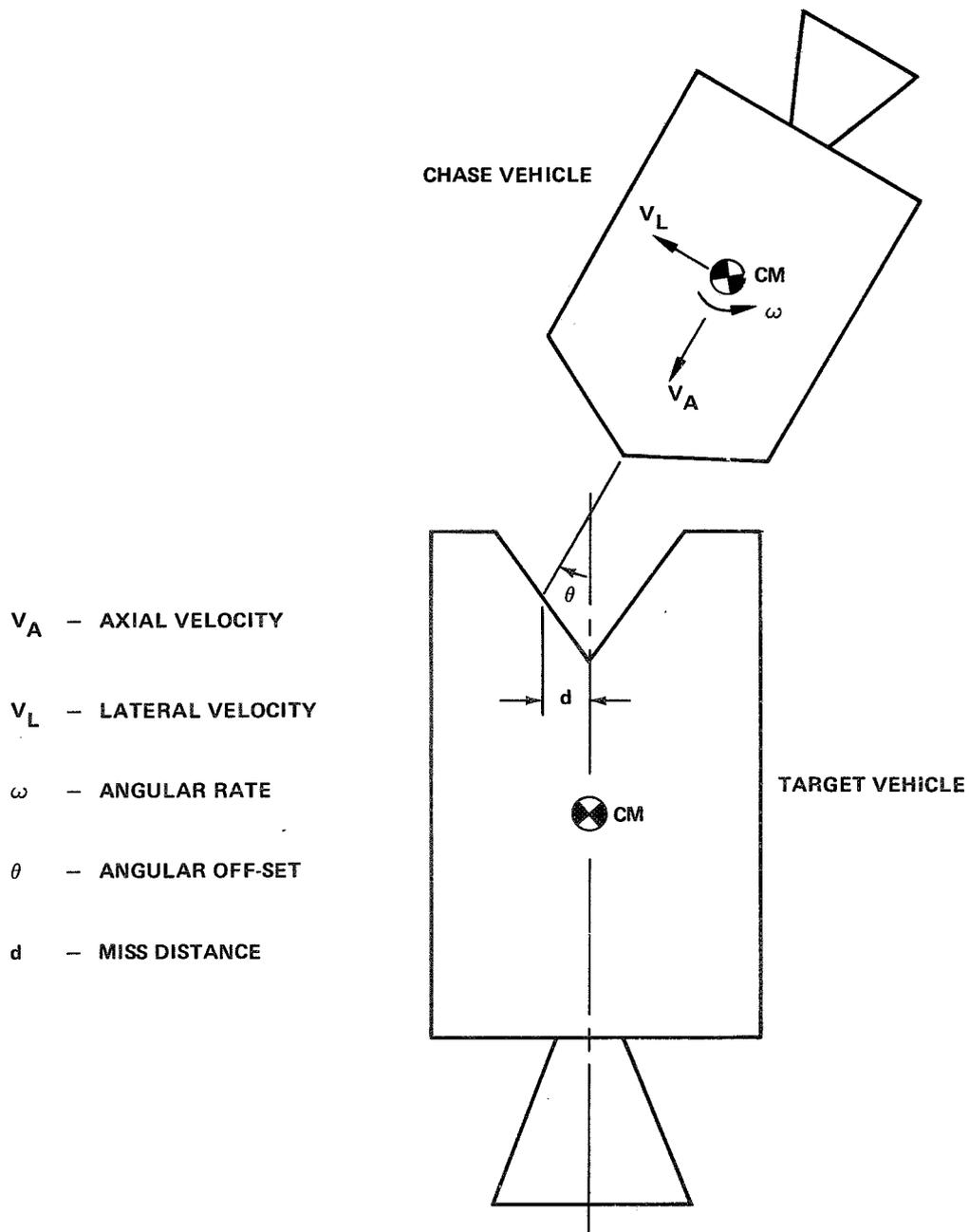
d — MISS DISTANCE

d

CM

TARGET VEHICLE

FIGURE 1 - INITIAL CONTACT PARAMETERS

friction to prevent slipping (relative sliding of the probe on the drogue) during all or part of the contact. Once computed, N* and F* are then applied to the chase and target vehicles to determine relative linear and angular rates after impact.

Since most captures occur in the slipping mode[1,6], it is necessary to compute a slip distance. However, the impulse-momentum method by itself cannot give the slip distance since it yields no information on the duration of contact, t_c.

A separate algorithm is therefore used to approximate t_c. By considering the mass properties of the vehicles and some experimental data on contact times [6], an effective spring constant of the probe-drogue contact surface was derived. Equations for t_c are based on this effective spring constant, mass properties of the vehicles, and thrust if present. The slip distance and disengagement point are determined from the slip rate during contact, duration of contact, and the original contact point.

Finally, by assuming a half-sine wave profile for the history of contact loads, the normal and friction forces are computed.

C. Kinematics After Impact

Once the disengagement point has been determined it is immediately checked to see if it represents a capture point. If the point does represent capture, the program prints "capture" and goes to the next case. If capture is not achieved, the program tracks the position of the probe tip relative to a coordinate system fixed at the apex of the drogue. Based on the velocity and angular rates of the vehicles after impact and a preselected time increment, successive positions of the probe tip are computed. After each time increment, the new probe location is checked to see whether the location represents capture, a missed attempt or a new impact. If a capture or a miss occurs, the appropriate message is printed and the program goes to the next case. If it is determined that there is a new impact, the problem is reinitialized by considering the required parameters just prior to impact as a new set of initial conditions. The aforementioned procedure is then reinitiated.

D. Capture Criteria

Capture criteria must satisfy both physical reality (to the highest degree possible) and reasonable ease of programming. As, previously noted, most captures occur in the slipping mode;

that is, while sliding during an impact. To account for this possibility, the slip distance during each impact is computed and it is determined if this slip distance is sufficient to carry the probe tip through the apex of the drogue. To anticipate a direct impact of the probe on the capture point, it is noted that there is a .0025 ft tolerance at the position where the probe head capture latches engage the drogue. This tolerance figure is adopted as a capture criterion in the following way: if an XY-coordinate system is set up at the apex of the drogue with the positive Y-axis outward along the drogue centerline, then capture is declared when the probe tip enters the region $Y < .0025$ ft.

E.   Missed Attempt Criterion

A missed attempt is declared whenever the probe tip position is located at $Y > 13.1$ inches (the depth of the drogue). This condition indicates the probe has left the drogue region. Missed attempts are also declared when the time interval between successive impacts exceeds a prescribed limit, say 10 seconds. The rationale for such a criterion is that after several impacts, the needed closing rate for a successful capture has been eliminated through energy dissipation and momentum exchange, and the vehicles are slowly drifting apart. Rather than wait for the probe tip to reach $Y > 13.1$ inches, time can be saved by declaring a miss and going on to the next case. Finally, when the number of impacts exceeds some limiting value, a miss is declared. It proved advantageous to adopt this criterion since the vehicles, while drifting apart, often make repeated contact along one side of the drogue surface.

F.   Subsequent Impacts

The drogue boundaries are defined by the equations

$$Y = \pm X \tan \beta$$

$$Y = 13.1$$

where β is the half-angle of the drogue. While tracking the probe tip after an impact, its position is first checked to assure $Y < 13.1$; if true, it is next determined whether the probe tip is within the drogue boundaries by examining the

inequality $-Y\cot\beta<X<Y\cot\beta$. If the X-position of the probe tip satisfies the inequality, a new position is computed based on the present position, velocity, and a prescribed delta in time. If it is determined that $X = \pm Y \cot \beta$ to 8 places (a highly unlikely event), impact is declared and the problem is reinitialized. More likely, it will be determined that the probe tip has overshot the boundary. In this event, the program backs up to the old position and, based on the velocity vector and distance from the surface, computes a new impact point.

G.   Attitude Control and Thrust During Docking

The simulation allows for adding attitude control and thrust to the chase vehicle and attitude control to the target vehicle during the docking maneuver. The chase vehicle in the AAP docking maneuvers is the CSM and therefore its Stabilization and Control System is employed in a 0.2 degree minumum deadband attitude hold mode with attitude and rate gains of unity. Two 100 lb thrusters, about 13 ft apart, are fired in opposite directions (2-jet couple) to produce the control torque.

Thrusting during the docking attempt is implemented by the aft-firing CSM reaction control thrusters, four of which are located around the periphery of the vehicle. Thus, a maximum thrust of 400 lbs is available. However, a command sharing logic must exist to take into account the fact that two of the thrusters may be firing in opposite directions to hold attitude; the total thrust then available is 200 lbs.

COMPARISONS WITH OTHER SIMULATIONS

Direct comparisons between SDØCK and other simulations (mathematical or test) are not straightforward with regard to contact time during a sliding capture and peak probe tip loads. SDØCK computes a contact time based on conditions just prior to the impact; if capture takes place during this contact time interval, SDØCK simply declares capture and prints out the aforementioned value of contact time. In the other simulations, post latching (successful docking) time is also counted as contact time. With respect to loads (forces), SDØCK assumes a half-sine wave profile while the other simulations compute or measure the profile. In addition, loads computed by SDØCK just prior to a sliding capture are based on the truncated value of contact time (see above) and are likely to be overestimated.

        With these considerations in mind, Table 1 presents
a comparison between SDØCK and two mathematical simulations and
one full-scale test simulation. The mathematical simulations*
are from North American Rockwell (NR) and NASA Manned Spacecraft
Center (MSC) while the full-scale docking simulation test (DST)
was done at McDonnell Douglas Aircraft Corp. - East (MDAC-E).
For Table 1, case (a), general agreement seems fair except for
peak load of the second impact and capture. These discrepancies,
however, can be explained. Under the initial conditions specified
for case (a), it is noted in the DST test report[6] that the
drogue skin was ruptured by the second impact. SDØCK predicts
a second impact probe tip load of 5568 lbs, approximately twice
the magnitude determined by the NR simulation and the DST.
The load measured by the DST should be lower because the
structural failure relieves the load. Furthermore, the
coefficient of restitution is radically altered since the
rupture causes an essentially plastic impact. SDØCK cannot
predict a structural failure and assumes a constant coefficient
of restitution. It is not understood how the NR simulation
agrees so well with the DST unless it can account for the
structural failure. The damage incurred by the drogue in the
DST case (a) precluded capture. The NR simulation also predicts
no capture. SDØCK predicts several subsequent impacts and,
with the assist of 400 lbs of axial thrust, eventual capture
9.5 seconds after impact.** Perhaps a more revealing picture
of the agreement between SDØCK and DST is shown in Figure 2
where the trajectory of the probe tip after initial contact
with the drogue is plotted. The effect of the ruptured drogue
on the DST trajectory is apparent. In Table 1, case (b),
agreement is again generally good although there exist some
problems. In the DST, the capture latches were found to be
damaged; otherwise capture would have been achieved since the
probe tip positioned itself in the drogue apex and remained
there.

        Figure 3 illustrates typical capture boundaries for
the lunar transposition docking case (see bottom of Table 1 for
vehicle properties). The solid curve was obtained by MSC and
the dashed curve by SDØCK. Agreement is seen to be quite good.
The curve obtained by SDØCK required 24 cases and ran in 16
seconds on the UNIVAC 1108.

_____

    * Results from mathematical simulations were obtained from
Reference 6.

    ** The DST fires its axial thrusters for only 4 seconds
after initial impact.

TABLE 1

CASE: LUNAR TRANSPOSITION DOCKING (MISSION D)[1]:
v_A = .898 F/S, v_L = .666 F/S, ω = -1.0°/S, θ = -10.0°, d = 10.52 in,
Axial Thrust (400 lbs)

		(SDØCK)	NR Mathematical Model	MDAC Test (DST)
Peak Loads (lbs)	Impact 1	2926	2832	2245
	Impact 2	5568	2750	2750
Time of Contact (secs)	Impact 1	.45	.45	.45
	Impact 2	.46	.54	.54
Capture	Yes or No	Yes	No	No (Drogue Damaged)
	Time to Capture	9.5 sec	NA	NA

(a)

CASE: LUNAR TRANSPOSITION DOCKING (MISSION D)[1]:
v_A = 1.0 F/S, v_L = -.5 F/S, ω = 0.0°/S, θ = 0.0, d = 9.13 in,
No Axial Thrust

		(SDØCK)	MSC Mathematical Model	MDAC Test (DST)
Peak Loads (lbs)	Impact 1	852	Only one component available (600 lbs, axial)	630
	Impact 2	3948	Only one component available (2000 lbs, axial)	2855
Time of Contact (secs)	Impact 1	.45	.50	.47
	Impact 2	Capture achieved on 2nd impact	⟶	?
Capture	Yes or No	Yes	Yes	No (Damaged Capture Latches)
	Time to Capture	1.2 sec	1.0 - 2.0 sec	NA

(b)

[1] Vehicle Properties: M_1 = 1840 slugs, M_2 = 6900 slugs

I_1 = 81000 slug·ft^2, I_2 = 2.34 x 10^6 slug·ft^2

INITIAL CONTACT POINT

TEST (DST)

SDØCK
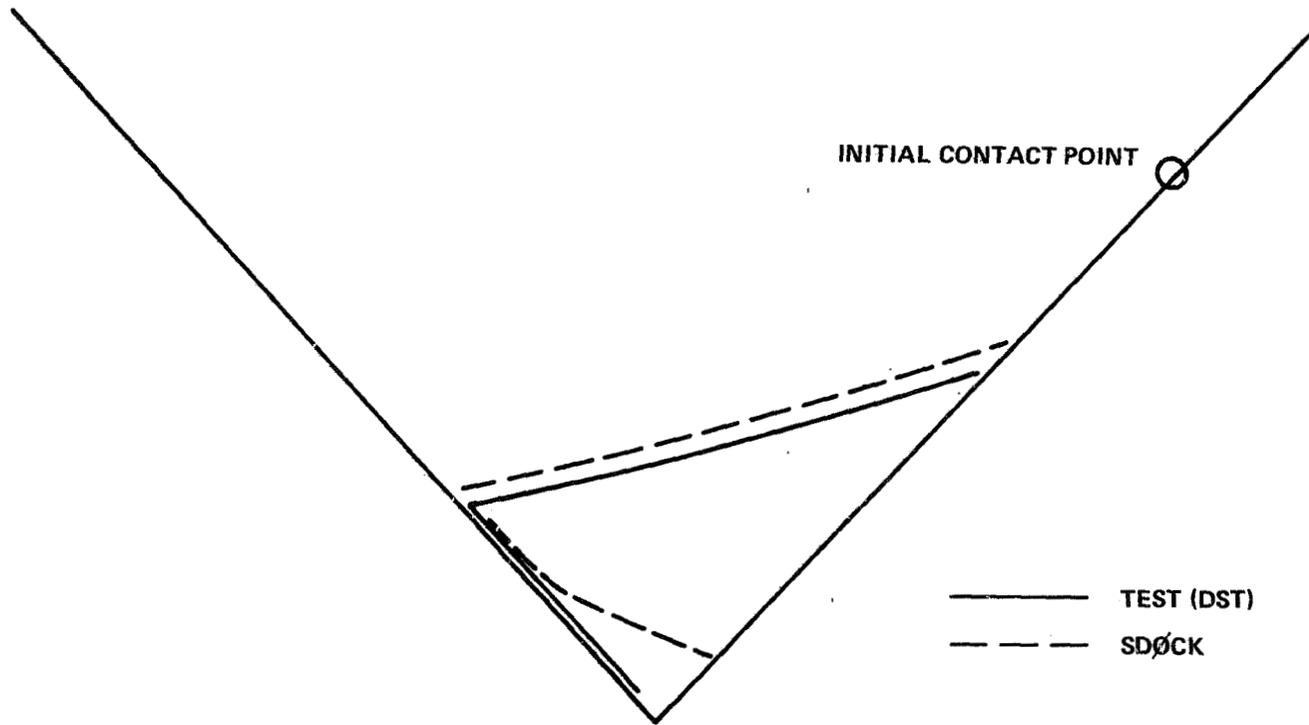
FIGURE 2—PROBE TIP TRAJECTORY

LUNAR TRANSPOSITION DOCKING (MISSION D)

THRUSTING	NO
ANGULAR OFF-SET, DEG	0.0
ANGULAR RATE, DEG/SEC	0.0
LATERAL VELOCITY, FT/SEC	0.2

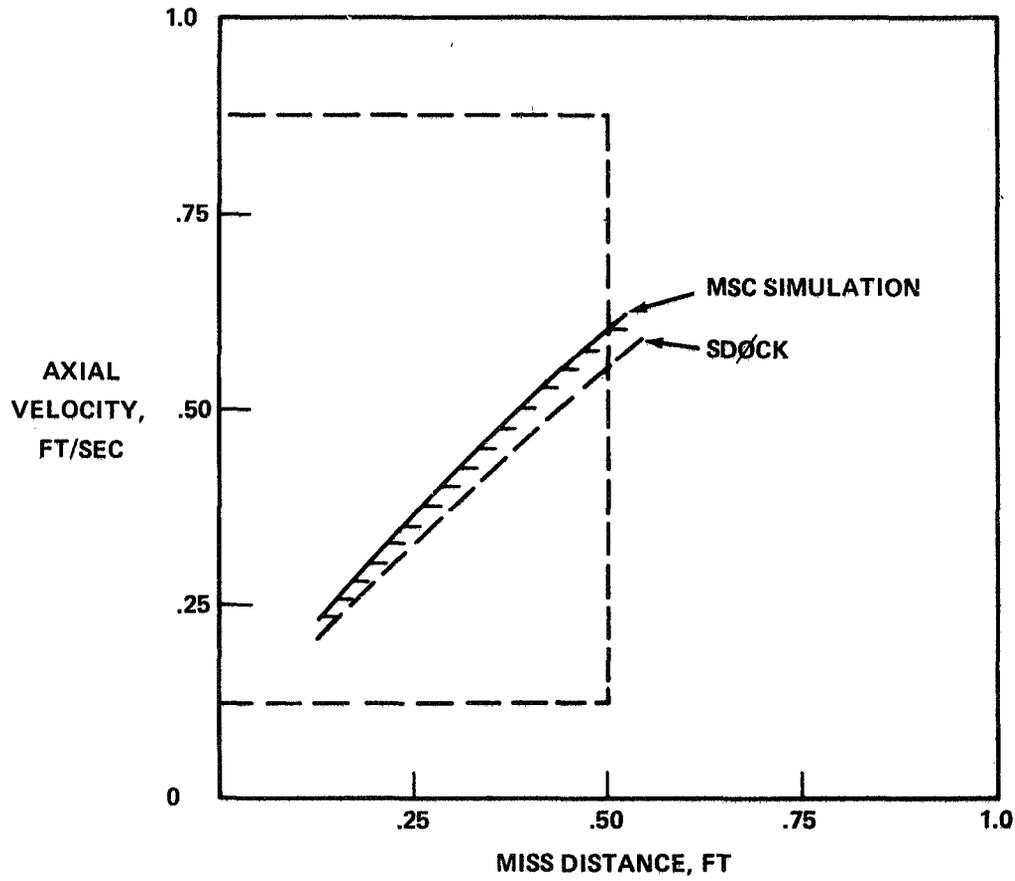LOW PROBABILITY OF CAPTURE
ON THIS SIDE

FIGURE 3—TYPICAL CAPTURE BOUNDARY

Based on these results, it is felt that the object of this study, namely the rapid production of accurate trends, has been achieved.

APPLICATION OF SDØCK TO AAP

The SDØCK docking simulation was applied to a comprehensive spectrum of cases (initial conditions) for axial docking of the CSM to the AAP-2 Payload.* Vehicle properties were obtained from Reference 7, and are listed here for convenience.

$$M_1 = 1084. \quad \text{slugs}$$

$$M_2 = 1799. \quad \text{slugs}$$

$$I_1 = 55202. \quad \text{slug-ft}^2$$

$$I_2 = 1182652. \text{ slug-ft}^2$$

The array of cases is defined as follows:

$$v_A (\text{ft/sec}) = 0.4, 0.6, 0.8, 1.0;$$

$$v_L (\text{ft/sec}) = 0.0, \pm 0.1, \pm 0.3;$$

$$\omega (\text{deg/sec}) = 0.0, \pm 0.5;$$

$$\theta (\text{deg}) = 0.0, \pm 5.0;$$

$$d (\text{ft}) = 0.25, 0.50, 0.75.$$

This represents a total of 540 sets of initial conditions. Additionally, each case was run with the following options:

   i)   attitude control with no axial thrust;

  ii)   attitude control with axial thrust;

 iii)   axial thrust without attitude control.

---

* The AAP-2 Payload consists of the Orbital Workshop, Multiple Docking Adapter, and Airlock Module.

Therefore, a total of 1620 simulated docking attempts were run. Twelve cases proved to be ill-defined (negative closing rate) so that the results will be based on 1608 cases. Note that two of the aforementioned options, (ii) and (iii) include axial thrust so that overall results are biased toward a more favorable prediction of capture. The reason for including options (ii) and (iii) was to assess the impact of sharing the total axial thrust available with the attitude control requirements in relation to assisting capture. Total UNIVAC 1108 computer time for the 1620 cases was about 19.5 minutes.

DISCUSSION OF RESULTS FOR AAP

Tables 2 through 5 provide a gross statistical breakdown of the results and illustrate immediately the effect of initial parameters and flight modes. Figures 4, 5, and 6 are the capture boundaries derived from the results and are a pictorial representation of the statistical results. Regions on the hatched sides of the curves represent regions of no capture or, at best, low probability of capture. Absence of any curves on the plots indicates capture included for all cases.

Table 2 presents the effect of thrusting and, in particular, the advantage of applying full (400 lb) axial thrust with no attitude control. For all values of initial parameters, the axial thrust (a/t)-no attitude control (a/c) option provided 80% successful captures in 537 attempts. This compares with 69% (out of 537 attempts) for the a/t and a/c mode and 52% (out of 534 attempts) for the a/c and no a/t mode. For the total 1608 valid attempts, there were 1073 successful docks (67% success). Table 3 illustrates the adverse affect of negative angular rates (ω). This is to be expected since negative angular rates cause higher probe tip velocity components normal to the drogue wall,*with correspondingly higher loads and greater rebound after impact. Positive angular rates provide for more glancing impacts. Table 4 confirms the intuitive impression that high positive off-set angles, θ, will have a deleterious effect on successful docking. This is to be expected since high positive off-set angles cause a higher proportion of the axial velocity to be directed normal to the drogue surface. It is apparent in each of Tables 2, 3, and 4 that increasing miss distance, d, causes a decreasing percentage of captures; this is an expected result. Table 5 illustrates the effect of initial axial velocity, v_A, and lateral velocity, v_L, on the

---

*Without loss of generality, all initial impacts are assumed to occur on the side of the drogue indicated in Fig. 1; hence, negative angular rates cause higher initial probe-tip velocities normal to the drogue wall.
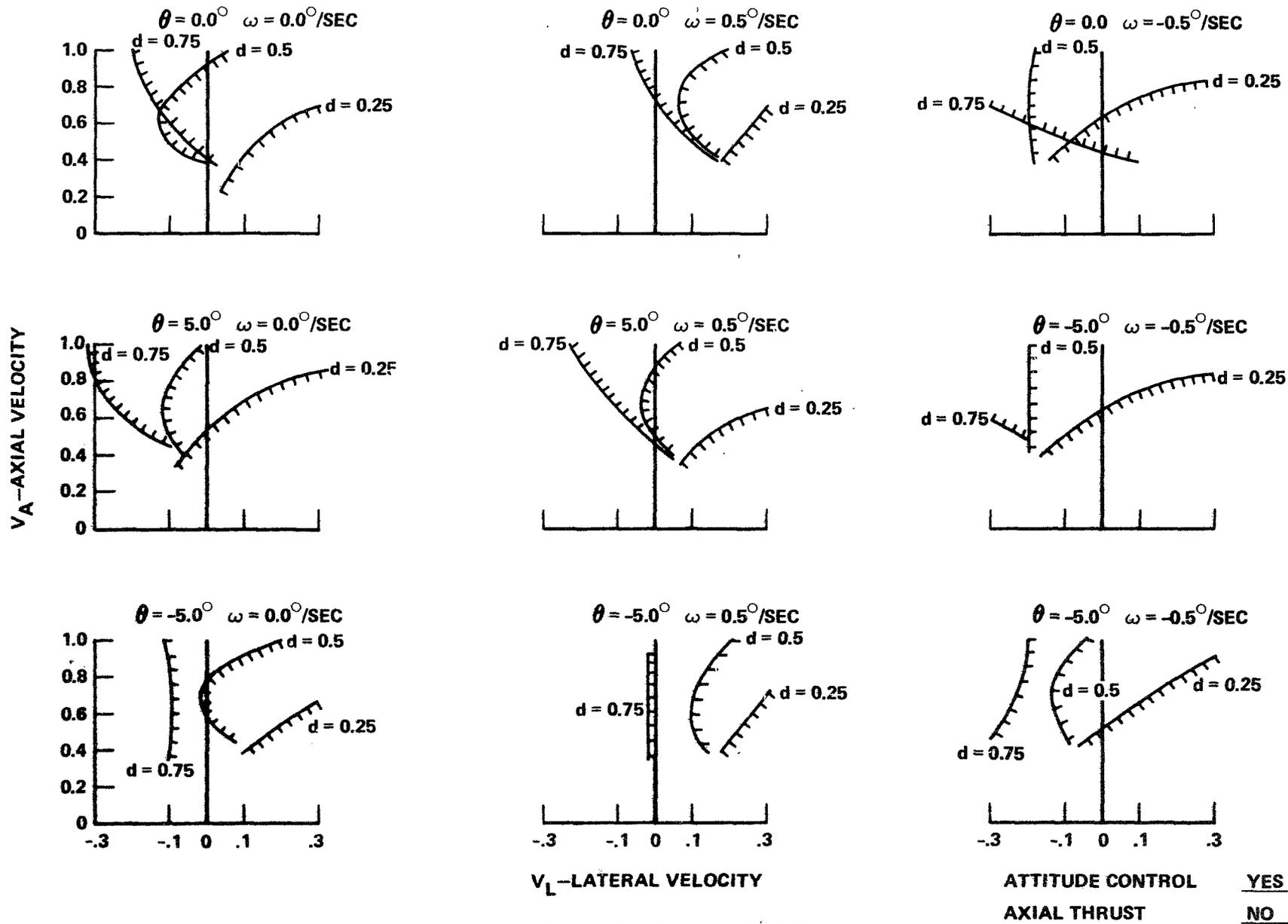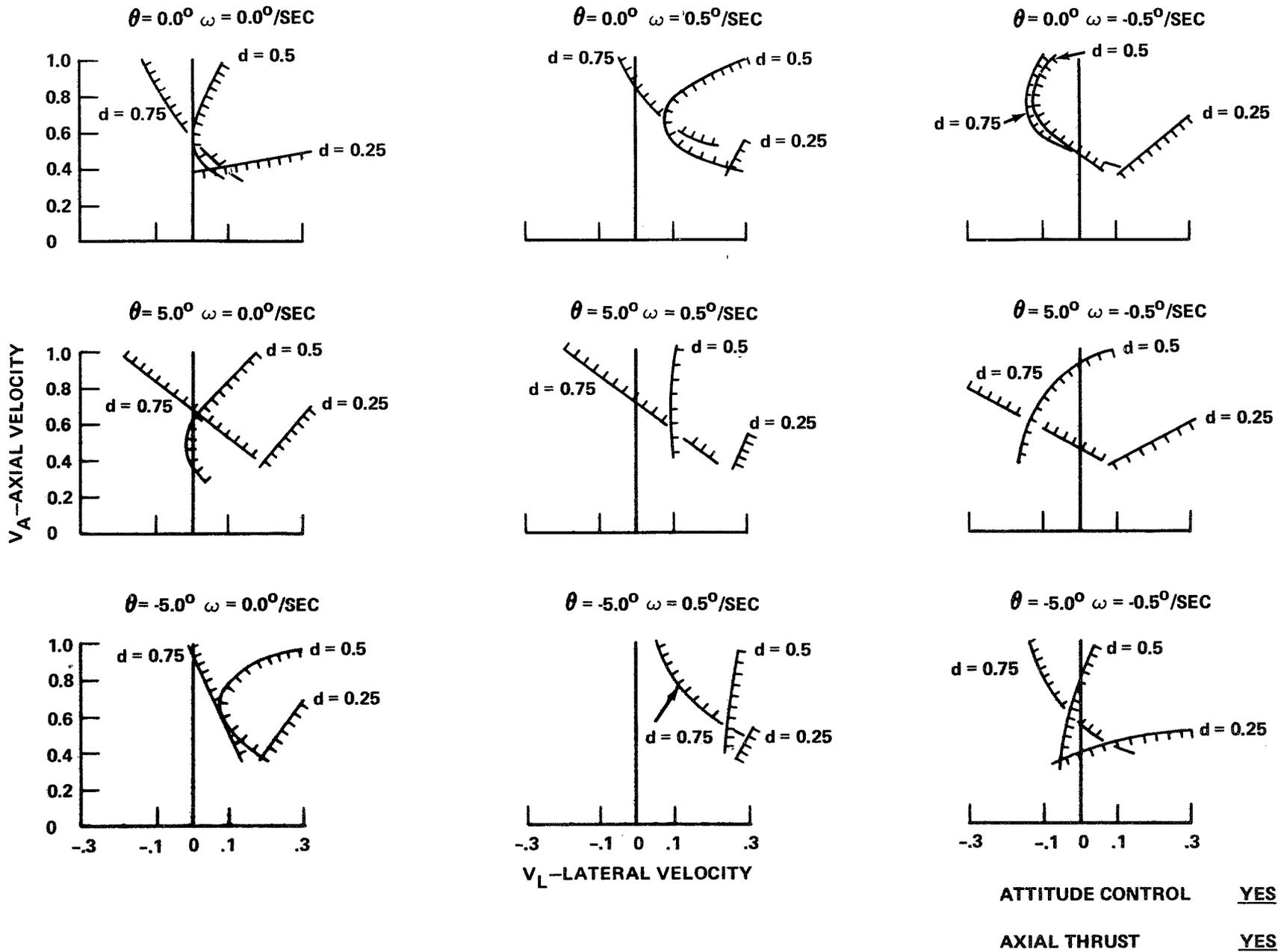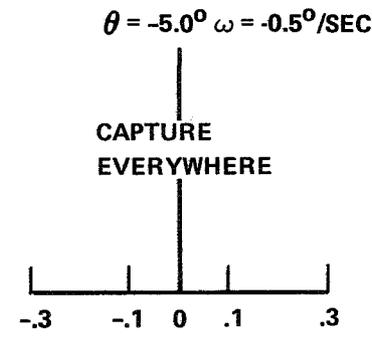
$\theta = 0.0^\circ$ $\omega = 0.0^\circ$/SEC

$\theta = 0.0^\circ$ $\omega = 0.5^\circ$/SEC

$\theta = 0.0$ $\omega = -0.5^\circ$/SEC

$\theta = 5.0^\circ$ $\omega = 0.0^\circ$/SEC

$\theta = 5.0^\circ$ $\omega = 0.5^\circ$/SEC

$\theta = -5.0^\circ$ $\omega = -0.5^\circ$/SEC

$\theta = -5.0^\circ$ $\omega = 0.0^\circ$/SEC

$\theta = -5.0^\circ$ $\omega = 0.5^\circ$/SEC

$\theta = -5.0^\circ$ $\omega = -0.5^\circ$/SEC

V_A—AXIAL VELOCITY

V_L—LATERAL VELOCITY

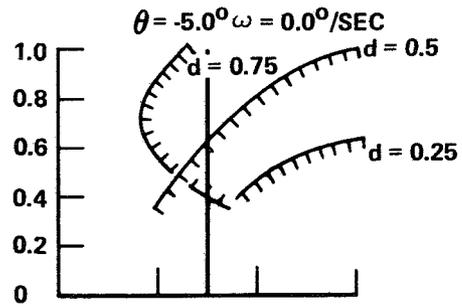| ATTITUDE CONTROL	YES
AXIAL THRUST	NO

FIGURE 4 - CAPTURE BOUNDARIES

FIGURE 5 - CAPTURE BOUNDARIES

FIGURE 6 - CAPTURE BOUNDARIES

		Attitude Control No Axial Thrust	Attitude Control And Axial Thrust	Axial Thrust Only
Range of Parameters	d	$\frac{\text{Captures}}{\text{Attempts}}$ (%)	$\frac{\text{Captures}}{\text{Attempts}}$ (%)	$\frac{\text{Captures}}{\text{Attempts}}$ (%)
$0.4 \leq v_L \leq 1.0$	0.25	137/178 (77%)	163/179 (91%)	166/179 (93%)
$-0.3 \leq v_L \leq 0.3$	0.5	83/178 (47%)	115/179 (64%)	141/179 (79%)
$-5.0 \leq \theta < 5.0$				
$-0.5 \leq \omega \leq 0.5$	0.75	58/178 (33%)	88/179 (49%)	122/179 (68%)
TOTALS		278/534 (52%)	366/537 (69%)	429/537 (80%)

TABLE 2

		$\omega = -0.5$ °/sec	$\omega = 0.0$ °/sec	$\omega = 0.5$ °/sec
Range of Parameters	d	$\frac{\text{Captures}}{\text{Attempts}}$ (%)	$\frac{\text{Captures}}{\text{Attempts}}$ (%)	$\frac{\text{Captures}}{\text{Attempts}}$ (%)
$0.4 \leq v_A \leq 1.0$	0.25	145/180 (81%)	159/180 (88%)	164/176 (93%)
$-0.3 \leq v_L \leq 0.3$	0.5	84/180 (47%)	117/180 (65%)	133/176 (76%)
$-5.0 < \theta < 5.0$				
All Axial Thrust and Attitude Control Options	0.75	65/180 (36%)	93/180 (52%)	116/176 (66%)
TOTALS		294/540 (54%)	369/540 (68%)	413/528 (78%)

TABLE 3

		θ = -5.0°		θ = 0.0°		θ = 5.0°	
Range of Parameters	d	$\dfrac{Captures}{Attempts}$	(%)	$\dfrac{Captures}{Attempts}$	(%)	$\dfrac{Captures}{Attempts}$	(%)
$0.4 \leq v_A \leq 1.0$ $-0.3 \leq v_L \leq 0.3$ $-0.5 \leq \omega \leq 0.5$ All Axial Thrust and Attitude Control Options	0.25	160/177	(90%)	157/179	(88%)	149/180	(83%)
	0.5	134/177	(76%)	112/179	(63%)	88/180	(49%)
	0.75	112/177	(63%)	95/179	(53%)	63/180	(35%)
TOTALS		406/531	(76%)	364/537	(68%)	300/540	(56%)

TABLE 4

v_A (ft/sec)	$\dfrac{\text{Number of Captures}}{\text{Number of Attempts}}$	v_L	$\dfrac{\text{Number of Captures}}{\text{Number of Attempts}}$
0.4	262/393	$v_L > 0$	293/648
0.6	251/405	$v_L = 0.0$	218/324
0.8	262/405	$v_L < 0$	564/648
1.0	298/405		
(a)		(b)	

TABLE 5

number of captures. Intuition would lead us to expect that increasing axial velocity would be beneficial (as long as loads are kept within structural limits). Table 5 (a), however, indicates that for $0.4 \leq v_A \leq 0.8$, there is relatively little improvement in the number of captures while for $v_A = 1.0$, there exists a moderate improvement. An examination of the capture boundaries in Figures 4, 5, and 6 show that for d = 0.25' the results coincide with intuition. However, for d = 0.5' and 0.75', the values of $v_A < 0.4$, and $v_A > 0.8$ appear more favorable. The reason for this, based on examination of the probe tip trajectories, is that for d > 0.25', increasing axial velocity leads to higher rebound velocity and hence an earlier second impact at a greater distance from the drogue apex. A lower axial velocity causes a delayed second impact at a point closer to the drogue apex, a more favorable position for capture. However, as v_A increased further ($v_A > 0.8$ ft/sec), greater slip distances and residual axial velocity asserted themselves and proved to be beneficial to capture. Table 5 (b) confirms the notion that increasing positive lateral velocity (v_L), causing higher velocity components normal to the drogue surface, is detrimental to capture.

CONCLUSIONS

It is felt that SDØCK provides a generally accurate assessment of the docking problems that can be anticipated in AAP. The results indicate that the most important factors in achieving capture (without axial thrust) are reducing the miss distance to about 0.25 ft and attempting to achieve a glancing rather than direct initial impact. The addition of axial thrust proved a significant advantage and, at larger miss distances, axial thrust without attitude control was significantly better than axial thrust with attitude control.

ACKNOWLEDGEMENTS

1022-RJR-ep   R. J. Ravera

APPENDIX

Equations governing the analysis of spacecraft docking dynamics will be presented here. We define the following variables and parameters.

$CM_{1,2}$	center of mass of vehicle 1,2
e	coefficient of restitution
F^*	friction impulse
$I_{1,2}$	moment of inertia of vehicle 1,2
$M_{1,2}$	mass of vehicle 1,2
N^*	normal impulse
$u_{1,2}$, $v_{1,2}$	velocity components of vehicle 1,2 (see Fig. A-1)
X,Y	coordinate system fixed to the drogue apex
(X_{M1}, Y_{M1}) , (X_{M2}, Y_{M2})	coordinates of $CM_{1,2}$
X_c, Y_c	coordinates of initial probe contact point with drogue
$x_{1,2}, y_{1,2}$	coordinate systems located at $CM_{1,2}$ (see Fig. A-1) which move with the CM's but do not rotate with the vehicles; also, distances from $CM_{1,2}$ to contact point (see Fig. A-2)
β	drogue half-angle
μ	coefficient of friction
$\omega_{1,2}$	angular rates of vehicles 1,2
$(\ )_{max}$	maximum of a quantity
$(\ )_X, (\ )_Y$	X,Y components of a quantity
$(\ )'$	quantity after impact

The initial parameters, v_A, v_L, ω, θ and d (Figure 1 of text) are easily related to the above defined quantities just prior to the first contact through the following equations (assuming the target vehicle is stationary):

$$
\left.
\begin{aligned}
X_c &= -d \\
\omega_1 &= \omega \\
u_1 &= v_A \cos(\beta+\theta) - v_L \sin(\beta+\theta) \\
v_1 &= -v_A \sin(\beta+\theta) - v_L \cos(\beta+\theta) \\
u_2 &= v_2 = \omega_2 = 0
\end{aligned}
\right\} \quad \text{(A-1)}
$$

The first of eqs. (A-1) indicates that, without loss of generality, all initial impacts will occur on side A of the drogue (see Figure A-1).

Impulse Momentum Relationships

For vehicle 1, the chase vehicle, it is noted from Figures A-1 and A-2 that the change in system momentum due to impact is given by

and

$$
\left.
\begin{aligned}
M_1(u_1' - u_1) &= -F^* \\
M_1(v_1' - v_1) &= N^* \\
I_1(\omega_1' - \omega_1) &= x_1 N^* + y_1 F^*
\end{aligned}
\right\} \quad \text{(A-2)}
$$

with $\qquad x_1 = (X_c - X_{M1})\sin\beta - (Y_c - Y_{M1})\cos\beta$

and $\qquad y_1 = (X_c - X_{M1})\cos\beta + (Y_c - Y_{M1})\sin\beta$

FIGURE A-1
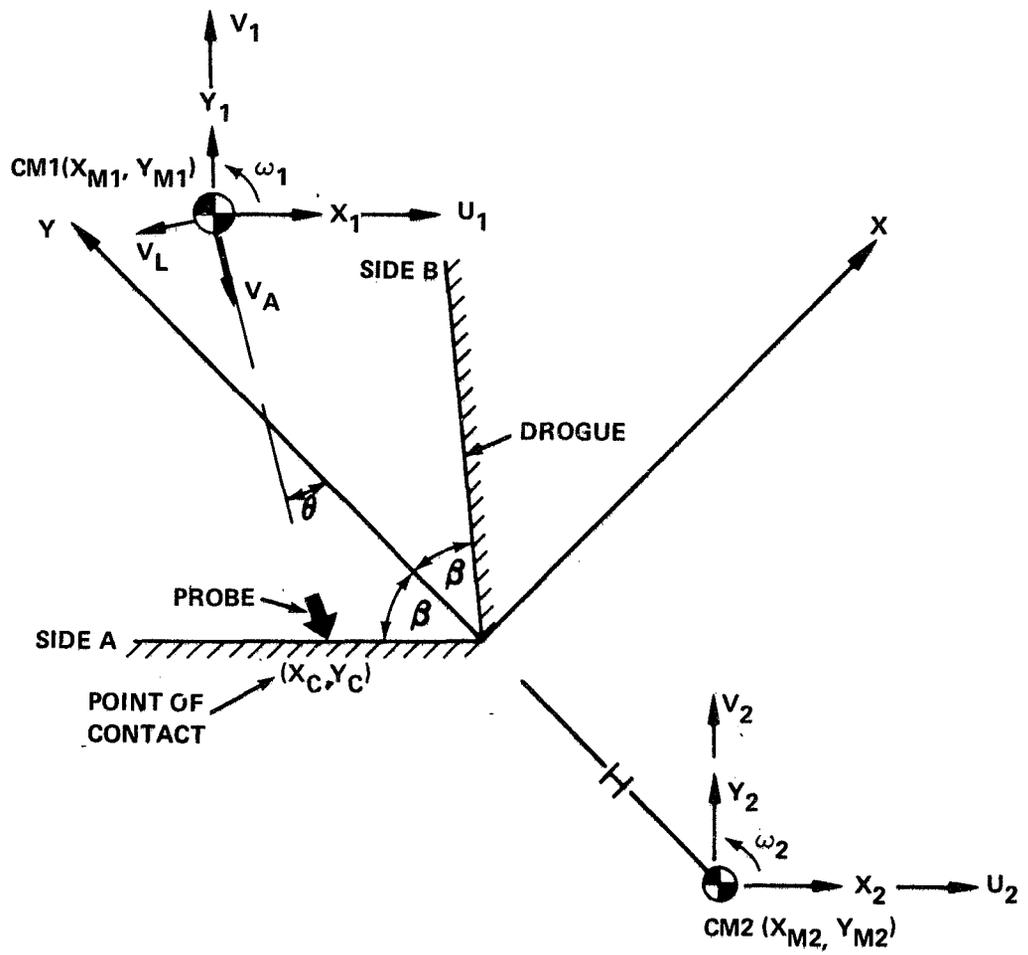

FIGURE A-2
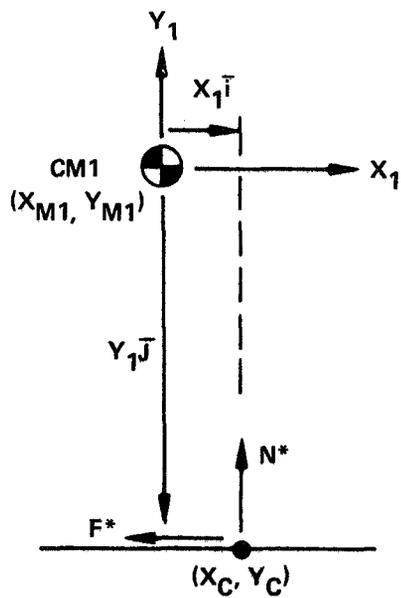
Similarly, for vehicle 2, the target vehicle,

$$M_2(u_2' - u_2) = F^*$$

$$M_2(v_2' - v_2) = -N^* \left.\begin{array}{c}\end{array}\right\} \qquad \text{(A-3)}$$

and $\quad I_2(\omega_2' - \omega_2) = -y_2 F^* - x_2 N^*$

with $\quad x_2 = (X_C - X_{M2})\sin\beta - (Y_C - Y_{M2})\cos\beta$

and $\quad y_2 = (X_C - X_{M2})\cos\beta - (Y_C - Y_{M2})\sin\beta$

Slip and Compression Rates

The slip rate, s, is defined as the velocity of the probe tip with respect to the drogue, in a direction tangent to the drogue surface at the point of contact (X_C, Y_C). The compression rate, c, is defined as the velocity of the drogue with respect to the probe in a direction normal to the surface at (X_C, Y_C). The slip rate before impact is

$$s = u_1 - u_2 - y_1\omega_1 + y_2\omega_2$$

and during and after impact

$$s' = u_1' - u_2' - y_1\omega_1' + y_2\omega_2' \qquad \text{(A-4)}$$

For the compression rate,

$$c = v_2 - v_1 + x_2\omega_2 - x_1\omega_1$$

and
$$c' = v_2' - v_1' + x_2\omega_2 - x_1\omega_1' \tag{A-5}$$

s' and c' can be expressed in terms of s, c, F^*, and N^* by combining eqs. (A-5) and (A-4) with eqs. (A-2) and (A-3); thus

$$s' = s - (B+E)F^* - AN^* \tag{A-6}$$

$$c' = c - AF^* - (B+D)N^* \tag{A-7}$$

where
$$A = \left(\frac{y_1 x_1}{I_1} + \frac{y_2 x_2}{I_2} \right)$$

$$B = \left(\frac{1}{M_1} + \frac{1}{M_2} \right)$$

$$D = \left(\frac{x_1^2}{I_1} + \frac{x_2^2}{I_2} \right)$$

and
$$E = \left(\frac{y_1^2}{I_1} + \frac{y_2^2}{I_2} \right)$$

Maximum Values of Normal and Friction Impulses

The values of the normal and friction impulses are dependent on the velocities before impact as well as the coefficients of friction and restitution. First, s' and c'

in eqs. (A-6) and (A-7) are set to zero, indicating that slip
or compression have ceased. This operation yields equations
for two lines,

$$(B+E)F^* + AN^* = s \qquad \text{(line ss)}$$

$$AF^* + (B+D)N^* = c \qquad \text{(line cc)}$$

which if plotted in an $F^* - N^*$ phase plane represent the zero
slip and compression rate lines. With the initial slip rate
$s>0$, the lines might appear as in Figure A-3(a). In this case,
F^* increases according to $F^* = \mu N^*$ as the vehicles make contact
and move until contact deformation is maximum (compression rate
is zero). When the compression rate is zero, the value of N^*,
N^*_c, is on line cc and is found by simultaneously solving

$$AF^* + (B+D)N^* = c$$

and
$$F^* = \mu N^* \; ;$$

the result is

$$N^*_c = \frac{c}{\mu A + B + D} \quad .$$

As the restitution phase procedes, F^* continues to increase
according to $F^* = \mu N^*$ since line ss is never intersected.
The maximum value of N^* therefore occurs at

$$N^*_{max} = (1 + e)N^*_c$$

In addition

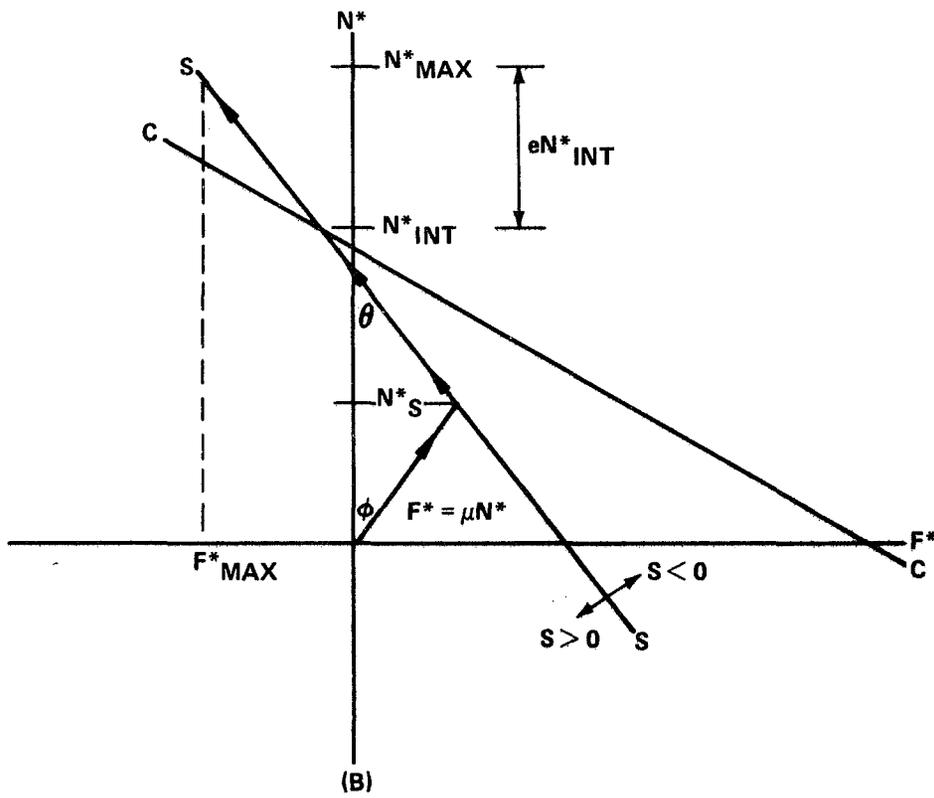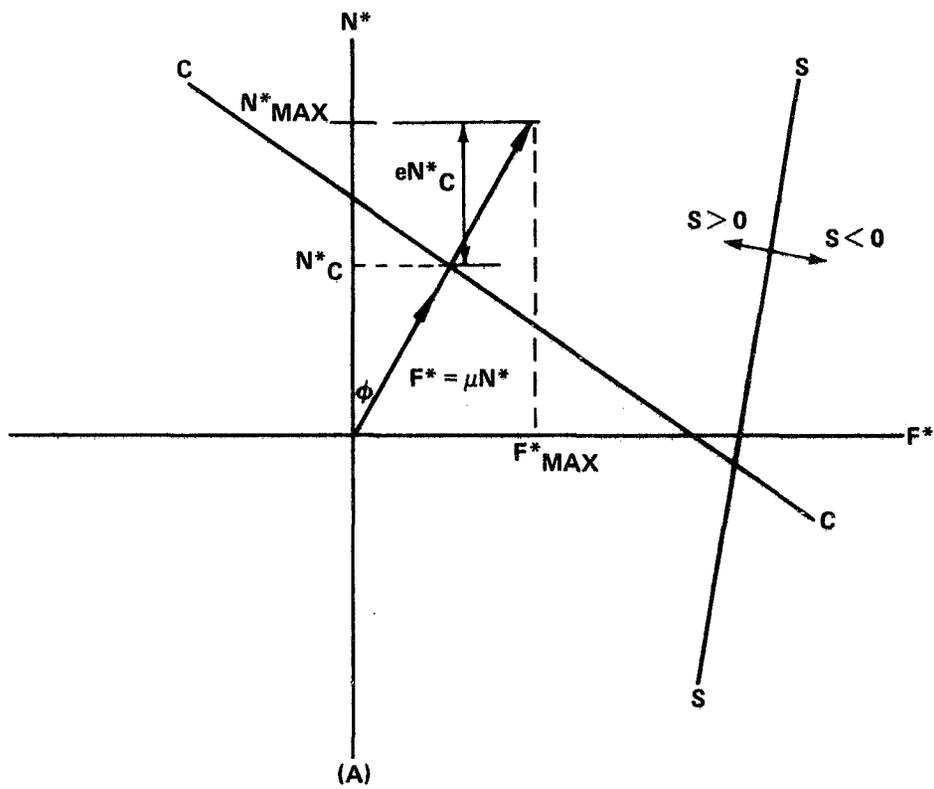$$F^*_{max} = \mu N^*_{max} \quad .$$

(A)

(B)

FIGURE A-3

The fact that the line ss is never intersected means there is not enough friction to bring the relative slipping between the vehicles to a stop.

Figure A-3(b) represents a different possibility. Zero slip rate is achieved before zero compression rate and slipping is halted. If there is enough friction to hold zero slip rate (determined by the condition $\phi = \tan^{-1}\mu \geq \theta$ in Figure A-3(b)) the motion procedes along ss, intersects cc, and continues until N^*_{max} is achieved. The intersection of ss with cc is given by

$$N^*_{int} = [(B+E)c - As]/[(B+E)(B+D) - A^2]$$

and

$$N^*_{max} = (1+e)N^*_{int} \quad .$$

Solving the appropriate geometry yields

$$F^*_{max} = (s - AN^*_{max})/(B+E) \quad .$$

All other possible alternatives are sorted out by the program and analyzed.

Approximate Value of Slip Distance

It is important to obtain an estimate of the amount of sliding that takes place during each contact since sliding is, by far, the most prevalent mode of capture. If a half-sine wave profile is assumed for the normal and friction forces, then

$$\left. \begin{aligned} N(t) &= N_{max}\sin \frac{\pi t}{t_c} \\[2em] F(t) &= F_{max}\sin \frac{\pi t}{t_c} \end{aligned} \right\} \qquad (A-8)$$

where t_c is the time the vehicles are in contact.* The impulses are, for any time during the impact, given by

$$
\left.
\begin{aligned}
N^* &= N_{max} \int_0^t \sin \frac{\pi t}{t_c} \, dt \\[2em]
F^* &= F_{max} \int_0^t \sin \frac{\pi t}{t_c} \, dt
\end{aligned}
\right\} \qquad \text{(A-9)}
$$

$$ t \leq t_c $$

Substituting (A-9) into (A-6), integrating with respect to time, and setting $t = t_c$ gives the maximum slip distance in the form

$$ d_s = st_c - \frac{(E+B)}{2} t_c F^*_{max} - \frac{At_c}{2} N^*_{max} \quad . $$

Recall that N^*_{max} and F^*_{max} are known from the previous section. Substituting $t = t_c$ in eqs. (A-9) gives an estimate for the maximum loads, N_{max} and F_{max}.

Contact Time

The contact time is approximated by considering the impact of the two vehicles (assumed rigid) having a spring at the point of contact. The spring may be assumed to represent

---

* An algorithm to compute t_c is explained later.

the stiffness of the probe and drogue along the normal to the drogue surface at the contact point. The contact time, t_c, will be computed by determining the half-period of the above mentioned model. The sping constant, k, is determined from experimental[6] and analytical[1] values of contact time. The equations for t_c are, without thrust,

$$t_c = \pi / \omega_e$$

where

$$\omega_e^2 = k \left(\frac{1}{M_e} + \frac{R_1^2}{I_e} \right)$$

with

$$M_e = \frac{M_1 M_2}{(M_1 + M_2)}$$

$$I_e = \frac{I_1 I_2}{\left(\frac{R_2}{R_1} \right)^2 I_1 + I_2}$$

and $R_{1,2}$ are the distances from the contact point (spring) to $CM_{1,2}$. With thrust,

$$t_c = \frac{2}{\omega_e} \tan^{-1} \left[\frac{M_e \omega_e c}{T_N} \right]$$

where T_N is the component of thrust normal to the drogue surface and it is recalled that c is the compression rate. Despite the obvious simplifications inherent in the model, good comparison is obtained with test and analytical results.[1,6]

Kinematics After Impact

In order to determine whether capture is achieved, it is necessary to track the position of the probe tip with respect to the apex of the drogue. From eqs. (A-2) and (A-3), the velocity components of the mass centers and angular rates of vehicles 1 and 2 are known. The X and Y components of the velocity of CM_1 with respect to the drogue apex, denoted by $(v_{1X})_2$ and $(v_{1Y})_2$, are found to be

$$(v_{1X})_2 = (u_1'-u_2')\sin\beta + (v_1'-v_2')\cos\beta + \omega_2'(Y_{M1}-Y_{M2})$$

(A-11)

and $\qquad (v_{1Y})_2 = (v_1'-v_2')\sin\beta - (u_1'-u_2')\cos\beta - \omega_2'(X_{M1}-X_{M2})$

If the instantaneous position of the probe tip with respect to the XY-coordinate system is represented by (X_p, Y_p) then the velocity components of the probe tip with respect to the droque apex are

$$(v_{pX})_2 = (v_{1X})_2 - (\omega_1'-\omega_2')(Y_p-Y_{M1})$$

(A-12)

and $\qquad (v_{pY})_2 = (v_{1Y})_2 + (\omega_1'-\omega_2')(X_p-X_{M1})$

The initial coordinates of the probe tip immediately after disengagement are determined from the contact point and slip distance; thus

$$X_p(\text{initial}) = X_c + d_s\sin\beta$$

(A-13)

and $\qquad Y_p(\text{initial}) = Y_c - d_s\cos\beta \ ,$

d_s being the aforementioned slip distance. Based on eqs. (A-12) and (A-13) and a selected time increment, a new position (X_p, Y_p) of the probe tip is computed. Effects of thrusting are added directly to eqs. (A-11) while attitude control firings are taken into account by adjusting the angular rates.

All the foregoing equations are based on a side A impact. For side B impacts, they are modified slightly because of the changes in directions of the normal and tangential components of forces and velocities with respect to the drogue wall (see Figure A-1).

BELLCOMM, INC.

REFERENCES

1. Personal Communication with J. A. Schliesing, Structures and Mechanics Division, MSC, March 12, 1969.

2. Brayton, W. D., "Dynamic Analysis of the Probe and Drogue Docking Mechanism," J. Spacecraft, V.3, N.5, May 1966, pp. 700-706.

3. Bodley, C., Holland, W. and Morosow, G. "A Method for Digital Computation of Spacecraft Response in the Docking Maneuver," ASME/AIAA 10th Structures, Structural Dynamics and Materials Conference (AIAA Volume), April 1969.

4. Routh, E. J., Dynamics of a System of Rigid Bodies (Elementary Section), Dover, 1960, p. 154.

5. CSM Technical Specification, Block II, SID-64-1344A, North American Aviation, November 22, 1966.

6. Preliminary Results of the McDonnell-Douglas Apollo Full-Scale Docking Simulation Test, Communicated by R. A. Garrett, MDAC-E, April 3, 1969.

7. "Mass Characteristics for the Cluster Mission," R-P&VE-VAW 69-37, MSFC, March 3, 1969.